# Momentum and Heat Transfer Processes in Recirculating Flows

# Momentum and Heat Transfer Processes in Recirculating Flows

*presented at*

THE WINTER ANNUAL MEETING OF
THE AMERICAN SOCIETY OF MECHANICAL ENGINEERS
CHICAGO, ILLINOIS
NOVEMBER 16-21, 1980

*sponsored by*

THE HEAT TRANSFER DIVISION, ASME

*edited by*

B. E. LAUNDER
UNIVERSITY OF MANCHESTER INSTITUTE
OF SCIENCE AND TECHNOLOGY

J. A. C. HUMPHREY
UNIVERSITY OF CALIFORNIA, BERKELEY

THE AMERICAN SOCIETY OF MECHANICAL ENGINEERS
United Engineering Center 345 East 47th Street New York, N. Y. 10017

Library of Congress Catalog Card Number 80-69192

# PREFACE

In 1904 Prandtl published the boundary layer equations and, thereby, firmly stamped the direction of research in fluid mechanics for the next sixty-five years. In Aerodynamics especially (a discipline that is intrinsically concerned with non-recirculating flows) the decomposition of the flow into an inviscid region bounded, near rigid surfaces, by thin viscous zones, proved such a powerful stimulus that it sustained decades of outstandingly successful theoretical and experimental work.

Yet, in contrast, only a relatively small proportion of the flows in and around Mechanical Engineering equipment are reasonably well described by the thin shear flow equations. Commonly flow recirculations are present, particularly in heat transfer equipment where a judiciously provoked separation is often found to raise substantially the level of heat transfer coefficient. Because the equations describing such flow phenomena are much more difficult to solve than the boundary layer equations, the contributions made by computational fluid mechanics to the design of Mechanical Engineering equipment has been correspondingly less than in Aeronautics.

By 1970 the predominance of thin shear flow studies had begun to weaken and the ensuing decade has seen a steady development of computational procedures for recirculating flow and the essential supporting experimental techniques. Although considerable progress has been made, however, it is clear that we are still nearer the beginning than the end in providing the necessary fundamental research basis in this area. Accordingly, to provide both a forum for airing current work and a springboard for further research, the K-8 Committee of the Heat Transfer Division decided to sponsor a session at the 1980 WAM on Momentum and Heat Transfer in Recirculating Flows. In fact, the response to the announcement of the session was so vigorous that two sessions have been scheduled at which the twelve papers contained in the present volume are to be presented. The papers span many of the current areas of work including: both computational and experimental studies; laminar and turbulent flows; and both steady and unsteady flow phenomena.

Our thanks are due to the authors for their cooperation in meeting the necessarily strict deadlines that had to be applied in producing this volume and to the following research workers in recirculating flows who provided critical reviews of the contributed papers: M. Abrams, B. Armaly, T. Azzazy, P. L. Betts, I. Cornet, J. W. Daily, F. Durst, T. Han, A. P. Hatton, F. Hurlbut, A. Iribarne, J. A. Laitone, P. LeQuere, T. Ota, G. Raithby, A. K. Runchal, F. S. Sherman, M. Sindir, H. T. Sommer, L. Talbot, S. P. Vanka, B. R. White, J. H. Whitelaw, P. O. Witze.

J. A. C. Humphrey, B. E. Launder
Session Chairmen

## CONTENTS

# REATTACHMENT LENGTH AND CIRCULATION REGIONS DOWNSTREAM OF A TWO-DIMENSIONAL SINGLE BACKWARD FACING STEP

**B. F. Armaly and F. Durst**
Institute of Hydromechanics
University of Karlsruhe, Federal Republic of Germany

## ABSTRACT

Laser-Doppler measurements of reattachment length behind a single backward facing step mounted in a two-dimensional test section are reported. The expansion ratio of the test section is 1.94:1 with the larger channel being 1.01 cm. This channel has an aspect ratio of 18:1. Results are presented for laminar, transitional and turbulent flow of air, $72 < Re < 8000$. These results show that the various flow regimes are characterized by typical variation of the separation length with Reynolds number. The results do not only show the expected primary zone of recirculation flow attached to the backward facing step but show additional regions of flow separations, on the upper and on the lower walls, that have not been previously mentioned in the literature. Velocity fields are presented at different positions below the step to provide a deeper insight of the flow structure and to demonstrate the special behaviour in this flow region. Preliminary flow predictions are presented and are compared with the experimental results.

## INTRODUCTION

The separation phenomena in internal flow caused by sudden changes in flow geometry is well known. The importance of such flows to engineering equipment has been stressed in many publications, e.g. see refs. [1 to 3] , and attempts have been undertaken to develop advanced experimental and theoretical techniques, e.g. see refs. [4,5] , to study carefully these separated flows. It is only recently that these techniques have reached the required stage of development so that they can be of immediate use in fluid mechanics studies of internal flow with regions of recirculation. In the past, most experimental studies relied on flow visualization techniques and/or heat and mass transfer measurements to obtain fluid mechanics information in separated flows. Althought the obtainable information was limited to what one might call integral flow parameters, several publications have become available for various flow geometries. Among these, the two-dimensional backward facing step has obtained particular attention due to its geometrical simplicity [6 to 9] . Relying on information for boundary layer flow behaviour, it was believed that this simple flow geometry should also yield a simple flow pattern showing a single separation region as sketched in Fig. 1. In most of the available work, the length of the separation region was thought to be only dependent on the step height and on the momentum thickness of the oncoming flow, e.g. refs. [7 to 9] . Other regions of detached flow were not measured and/or have not been reported so far.

The present research work was carried out to deepen the existing understanding of internal flow with separation regions by measurements of velocity over a wide Reynolds number range covering laminar, transitional and turbulent flows. A laser-Doppler anemometer was employed to quantitatively define the variation of separation length with Reynolds number and to obtain detailed information on the velocity profiles downstream of the step. The experimental study showed additional regions of recirculating flow that have not been previously reported in literature. These regions exist on both walls of the test section and in the immediate vicinity of the reattachment point of the main separation region. Such regions will strongly influence the heat and mass transfer from these walls and were measured in details in this study.

The paper also presents preliminary numerical predictions of the reattachment point for this flow in the laminar region which are compared with experimental results. Good agreement is obtained between experimental and theoretical results. This is taken as a demonstration of the reliability of the employed numerical technique to study internal flows with separation in the laminar region. The authors' research work is continued with these techniques and extensions to separated flows with heat transfer are under way.

## APPARATUS AND EXPERIMENTAL PROCEDURE

The open loop air driven channel which was used for this study is shown schematically in Fig. 1. It incorporated a backward facing step that provided an expansion ratio of 1.94:1. The larger channel, downstream from the step has a height of 1.01 cm and an aspect ratio of 18:1. The tunnel and the test section were constructed from Aluminium and all the parts were machined to very close tolerances regarding paralleling of walls, surface roughness, manufacturing of step corners, etc. The two side walls were made of glass, 1 cm thick, to facilitate laser-Doppler measurements in the forward scattering mode. The air flow into the tunnel

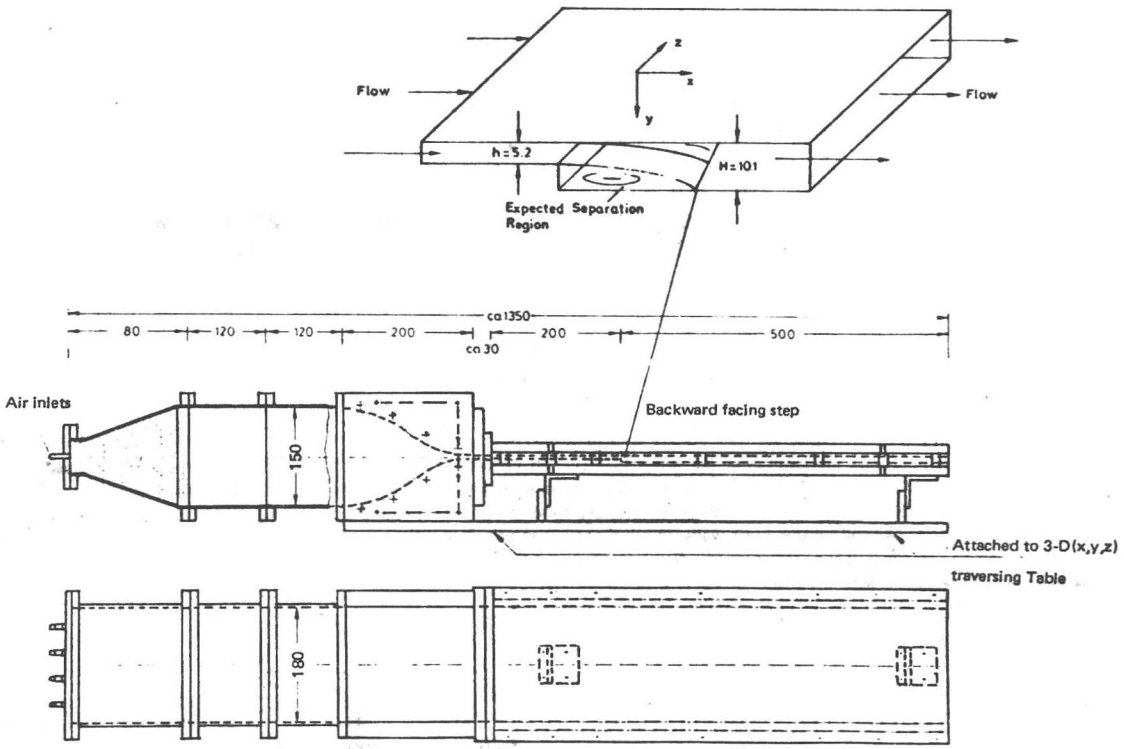


Fig. 1 Schematic of apparatus

contained scattering particles and was fed through five, 6 mm, bored tubes into the first part of the test section which had an expanding cross section and was packed with steel wool. The flow also had to pass through a section with flow straighteners and was then guided into a smooth contracting nozzle with an area ratio of 30 : 1. This nozzle was connected to the inlet of the test section which was 0.52 cm in height and 20 cm in length. These dimensions insured a two-dimensional fully developed flow at the cross section where the step was located. Each of the lower and the upper walls of the test section was machined from one Aluminium plate, 2 cm thick. The two plates and the glass side walls were held parallel together and were attached to the nozzle exit by location pins and held by machine screws. The assembly of channel and inlet section was placed on the top of a three-dimensional traversing table which allowed the measuring position to be located to within 0.1 mm in the x and z-direction and to within 0.01 mm in the y-direction. Dimensions of the tunnel and the test section with the coordinate system used in this study are shown in Fig. 1.

The air that was fed to the tunnel originated at a compressor and passed through a pressure regulation system which allowed the flow rate to be maintained constant to within 3 % over the complete run of one experiment. Before entering the expanding and contracting inlet section, the compressed air passed through a number of silicon-oil atomizers which ran in parallel to seed the air with silicon-oil particles of approximately 2$\mu$ in mean diameter. The seeded air passed through a settling chamber to remove the larger particles and was then guided to the test section. A schematic diagram with detailed description of this seeded air supply is given by Cherdron et al. [10] .

The laser-Doppler anemometer employed in the present investigation was operated in the fringe mode with optical arrangements similar to that used by Cherdron et al. [10] . It was employed in the forward scattering mode and was set up to measure only the x velocity component, that is parallel to the channel walls. It consisted of a 15 mW He-Ne-laser, an integrated although modular transmission optics with Bragg cells, light collecting optics with photomultiplier and signal processing equipments corresponding to the block diagram of Fig. 2. Two frequency tracking demodulators (BBC-Goertz "LSE01" and Cambridge Consultants "CC04") were initially used to process the Doppler signals. These two trackers proved to be incapable of properly tracking the Doppler signals for Reynolds number larger than 2000 in the neighbourhood of the reattachment zone. This was due to high turbulence levels in that region and the observed deterioration of signal quality very near to the wall. For that reason the Biomation transient recorder was used to digitize and store the signals from the photomultiplier. These signals were processed by a Hewlett Packard Computer to yield the required Doppler frequency of individual bursts and to compute from these the time averaged velocities. All the results which are presented in this study were processed via this latter digital processing scheme. A more detailed discussion of this Doppler signal processing scheme is given by Durst and Tropea [11] .

In order to obtain information on velocity profiles, the

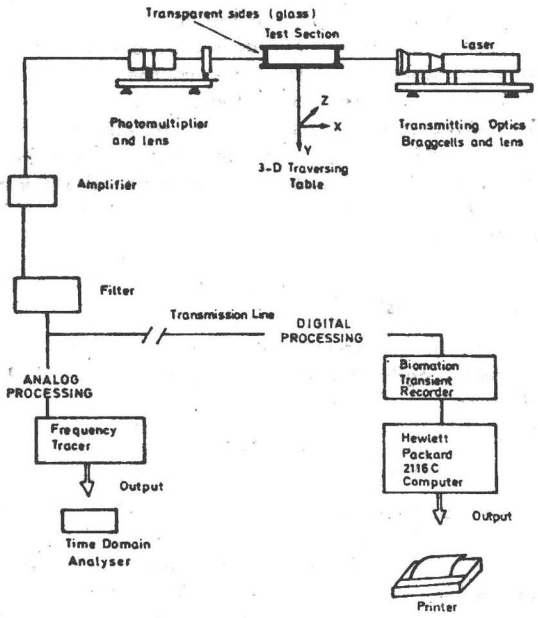


Fig. 2 Data acquisition and processing system

optical system was spatially fixed and the test section was moved, via a three-dimensional traversing table. This table was of high precision and permitted the measuring control volume to be placed at any desired location within the flow field. All of the measurements in this paper were made at the centre of the channel, $z = 0.0$, where the flow was shown to be nominally two-dimensional. Flow rates were varied by adjusting one of the regulating valves. For each flow rate, the Silicon-oil particle rate was also adjusted to insure a sufficiently high particle concentration for each flow rate that permitted proper processing of the Doppler signals. To measure the reattachment length at a given flow rate, the inlet velocity was measured to determine the Reynolds number and then the lower and the upper walls were scanned to determine the reattachment length and the presence of additional circulation regions behind the step. For a given measurement of local time mean velocity, 100-500 Doppler bursts with each having at least 20 cycles, were processed and averaged. The Biomation transient recorder was externally triggered at a rate slower than the occuring Doppler bursts to eliminate biasing. A time of 1 - 5 minutes was needed for each measuring point to gather and process the required number of Doppler bursts. To obtain the cross sectional velocity profiles, readings were taken at predefined locations in the test section. They were adjusted by means of the traverse table. The latter was also employed to determine the location of recirculating flows.

## RESULTS AND DISCUSSION

Measurements of the reattachment length and velocity distribution were performed for a Reynolds number range between 72 to 8000 which covered the laminar, transition and part of the turbulent regimes of the backward facing step flow. The definition of the Reynolds number which is used in this study is given by :

$$Re = V D/\nu \qquad (1)$$

where V is the average inlet velocity based on the measured maximum inlet velocity and the assumed fully developed parabolic profile, D is the hydraulic diameter of the inlet, small, channel and is equivalent to twice its height, $D = 2h$ and $\nu$ is the kinematic viscosity. In all of the cases that are reported here, the average velocity was determined from measurements of velocity at the centre of the inlet channel at about 1 cm upstream of the step. Other Reynolds numbers used in step flow studies such as the one based on centre velocity and/or step height, can be easily deduced from the stated definition.

The assumption of two-dimensional flow and fully developed parabolic velocity profile in the inlet channel was confirmed by measurements. The flow in the plane of the sudden expansion in the inlet channel was symmetric and two-dimensional over the centre 12 cm of its width to within 1% as shown in Fig. 3. Also the velocity, in the laminar range, was fully developed with parabolic profile in the inlet channel as shown in Fig. 4. As expected (in the laminar range) for the flow with the higher Reynolds number a longer distance downstream from the step is required to become fully developed again, i.e. to reach a parabolic profile. This fact is demonstrated in Fig. 4 for two Reynolds numbers. The figure shows small deviations from the parabolic profile at the higher Reynolds number.

Measurements of reattachment length are shown in Fig. 5 as a function of the Reynolds number. From the shape of this curve one can clearly identify the laminar, $Re < 1200$, the transition, $1200 < Re < 6600$, and the turbulent, $Re > 6600$, regimes of the flow. To the authors' knowledge this is the first detailed measurement, via laser-Doppler anemometer, of reattachment length variation with Reynolds number that covers the three different regimes of flow and defines it on the basis of actual velocity measurements. Previous studies of this property have been carried out by means of flow visualization techniques or were performed on the basis of heat and mass transfer measurements [12 - 14] . The diffusive behaviour of these measuring techniques masks and smoothes any sharp gradients in the distribution. Further-

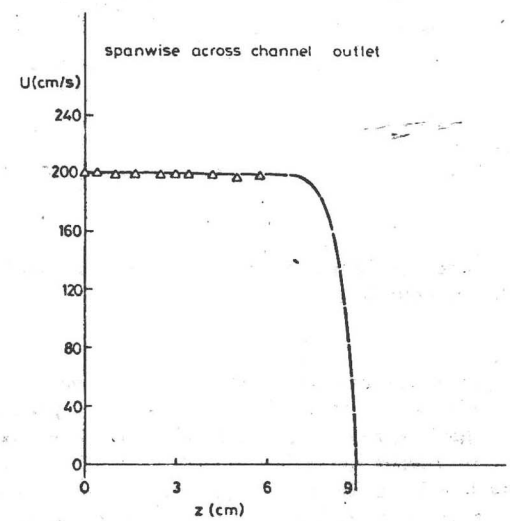


Fig. 3 Spanwise velocity distribution at the centre of the inlet channel

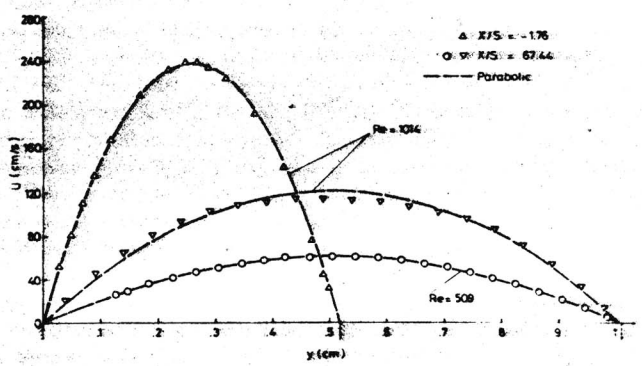


Fig. 4 Velocity profile in small and large channels

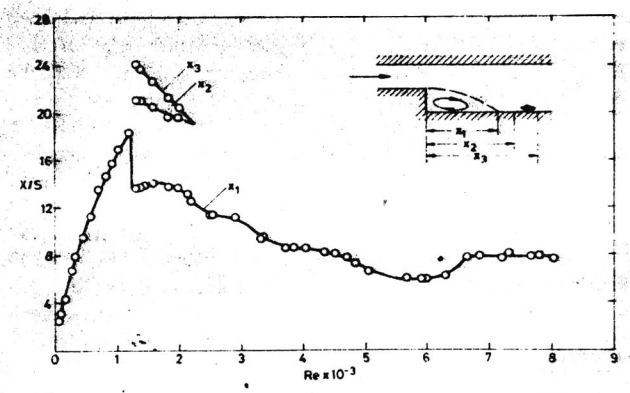


Fig. 5 Reattachment length and circulation region on lower wall

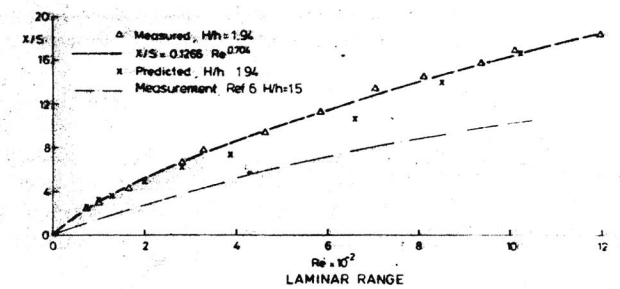


Fig. 6 Comparison between measured and predicted reattachment length

more, in previous studies detailed local measurements could not be performed accurately in the transition region.

The laminar regime of the flow is characterized by an increasing reattachment length with Reynolds number. This behaviour is not linear as suggested from measurements and predictions on other flow geometries (axisymmetric). This fact has also been demonstrated by Denham and Patrick [6] who reported only on laminar flow in a similar geometry but with expansion ratio of 3 : 2. Their resulst are presented in Fig. 6 and indicate a shorter reattachment length. When the two experimental results, present measurements and these of Denham and Patrick [6], are plotted versus a Reynolds number that is based on the step height and average velocity, $Re_s = Vs/\nu$, the two curves in Fig. 6 collapse into one curve indicating similarity between the two flow geometries. This fact indicates that at least in the laminar region one can use the results from this study to estimate the reattachment length in a similar geometry but with different expansion ratio and step height. The variation of separation length in this study is exponential and could be described by the following relation:

$$x_{1/s} = 0.127\, Re^{0.71} \qquad (2)$$

as shown in Fig. 6 where s is the step height and $x_1$ is the reattachment length. In terms of $Re_s$, equation (2) becomes equivalent to

$$x_{1/s} = 0.2\, Re_s^{0.71} \qquad (3)$$

This figure also includes some predictions of the reattachment length which were carried out by a Computer Code TEACH utilizing 25 x 27 grid points. Agreements are very good for low Reynolds number $Re < 300$. The authors are presently working on increasing the number of grid points in the flow domain and hope that this will also produce good agreement at the larger Reynolds numbers.

The regime of transitional flow $1200 < Re < 6600$ is characterized by first a sharp decrease in the reattachment length, a continued gradual, but irregular, decrease to a minimum value at Reynolds number of 6000, then followed by increase to a constant level which characterizes the turbulent flow regime. An interesting region of additional circulation was measured downstream of the primary region of separation and its extension is shown in Fig. 5. This additional region of circulating flow has not been previously reported in the literature. It is very thin and close to the wall, approximately 0.4 mm. It originates in the Reynolds number range corresponding to the early part of the transition region, see Fig. 5, where the reattachment length experiences a sharp drop in its magnitude. In this range strong vortex formations are expected in the flow and the additional region of circulation is believed to be due to vortex shedding from the edge of the step. These vortices approach the wall and the second recirculation region might be due to to the sharp change in flow which the eddies experience. Fig. 5 shows that the length of this secondary recirculation region decreases rapidly with Reynolds number and it disappears for Reynolds numbers larger than 2100. This region might be similar to the one observed by Sparrow and Kaleis [14] in their mass transfer measurements. Computer codes for predicting the behaviour in this region of the flow do not exist at present, and need to be developed. The use of a time dependent solution that follows the development of the flow might prove to be useful in this region. Initial work has been started along these lines at the University of Karlsruhe.

The turbulent range, $Re > 6600$, is characterized by a constant reattachment length. The measured value in that region is in agreement with the one measured by Abbot and Kline [1] for a similar test section geometry. Available Computer codes have been applied in turbulent separated flows and appear to predict measured values successfully in this region.

An additional recirculating flow region was measured at the upper wall downstream of the expansion as shown in Fig. 7. This region has also not been reported in the literature. It develops in the laminar range and remains in existance throughout the transition region. It develops due to the adverse pressure gradient created by the sudden expansion and its existance is believed to be dependent largely on the expansion ratio. Corresponding studies to confirm this are under preparation at the University of Karlsruhe. As Fig. 5 shows this circulation region disappears in the Reynolds number range that corresponds to the end of the transitional flow regime. The presence of this region of recirculating flow on the wall opposite to the step was also measured at the low Reynolds number but specifying accurately its starting and ending points is quite difficult. The authors believe that its length should start to decrease as the Reynolds number decreases and it should disappear below a certain value of Reynolds number. The existing Computer Code TEACH, predicts the existance of this circulation region at the upper wall but additional grid refinements are needed to precisely locate its starting and ending points. This work is presently undertaken by the authors parallel to velocity measurements in the lower Reynolds number range.

Fig. 8 summarizes the locations of the three circulation regions that were measured for test section geometry given in Fig. 1. It clearly demonstrates that for the majority of the measured Reynolds number range the beginning of the recirculation region at the upper wall is upstream from the reattachment point of the primary recirculating flow region and its end is downstream from it. Detailed velocity field measurements for this flow geometry is in progress and available results are presented to demonstrate clearly the interesting features of this separated flow. The velocity scan at a distance of 0.6 mm away from the upper wall for Reynolds number of 1014, which is in the laminar flow regime, is presented in Fig. 9. The velocity along that plane decreases rapidly with distance away from the step and it becomes negative at $x = 7.6$ cm. At $x = 12$cm the region with negative velocity ends and positive velocity occurs again beyond that point. Cross sectional velocity profiles at four positions for the Reynolds number of 1014 are presented in Fig. 10. The inlet, $x/s = -1.76$, and the far downstream, $x/s = 67.44$, profiles for this flow rate were shown in Fig. 4 and have been discussed. The two remaining profiles were taken at positions where only one recirculation region exists, i.e. $x/s = 7.04$ and $x/s = 19.04$. The first demonstrates the regular separation region behind the step and the second demonstrates the separation region on the upper wall. Figs. 9, 10 and 5 show clearly the thickness and length of these two circulation zones and provide information on the velocity field in them. Similar

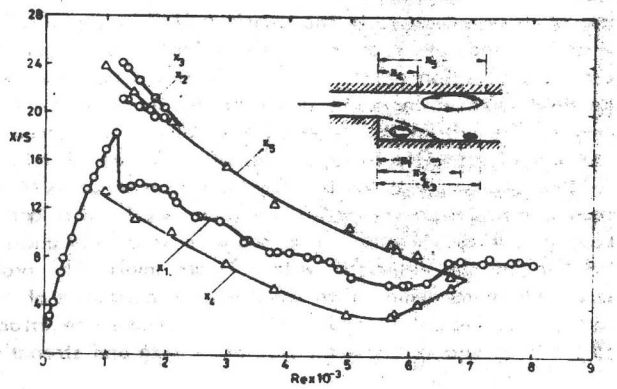


Fig. 8 Circulation regions at the upper and lower walls

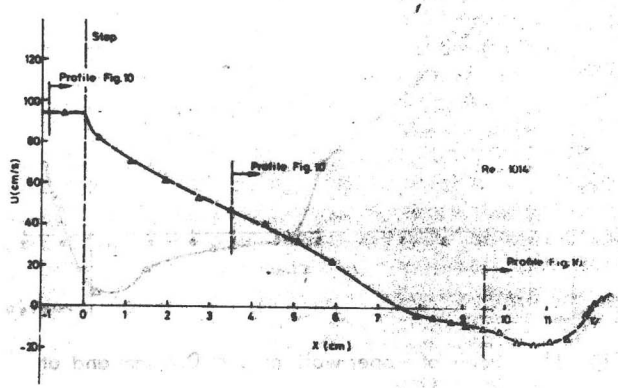


Fig. 9 Scan of upper wall at y = 0.6 mm and at Re = 1014

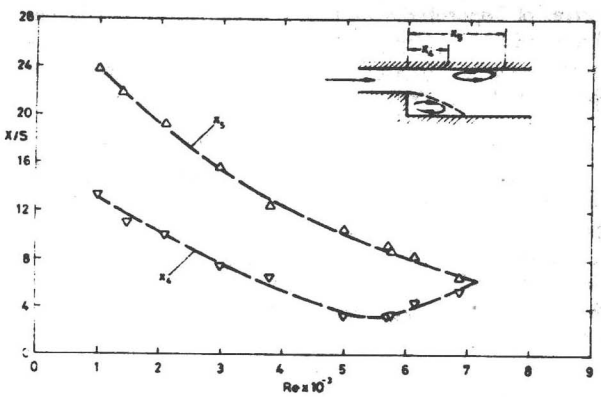


Fig. 7 Domain of circulation at the upper wall

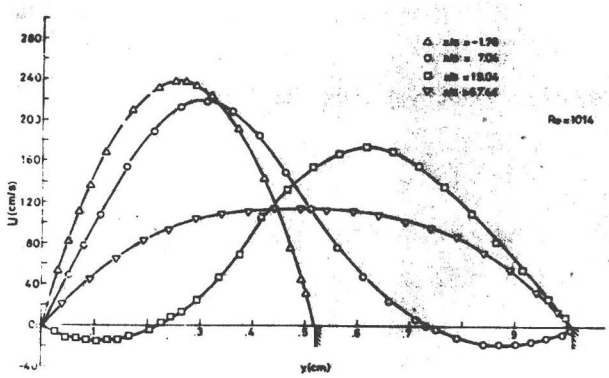


Fig. 10 Velocity profiles at various positions, Re = 1014

results are presented in Figs. 11 and 12 for Reynolds number of 1474 which is in the transitional flow regime. Figs. 9 and 11 indicate that in the transitional flow regime the circulation region on the upper wall moves upstream as the Reynolds number increases and that the shape of the velocity profile within it is skewed towards the downstream end. The velocity profile for x/s = 20.84 is presented in Fig.12. At that position and for the Reynolds number of 1474 the second circulation region on the lower wall exists and as seen from Figs. 12 and 5 it occupies a relatively small volume and the velocities within it are small. The profile is presented to demonstrate simultaneous existance of two circulation regions in addition to the primary one attached to the step and to show their relative size and strength.

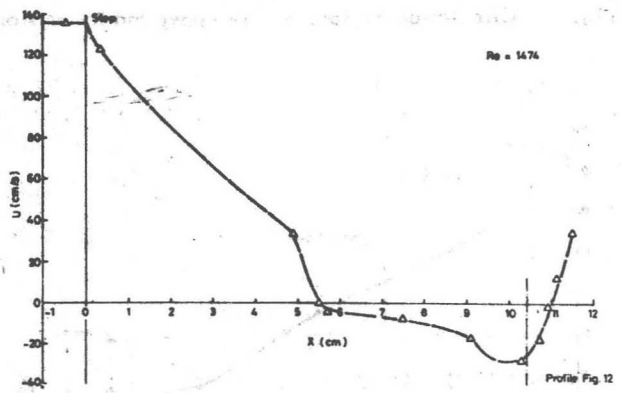


Fig. 11 Scan of upper wall at y = 0.6 mm and at Re = 1474

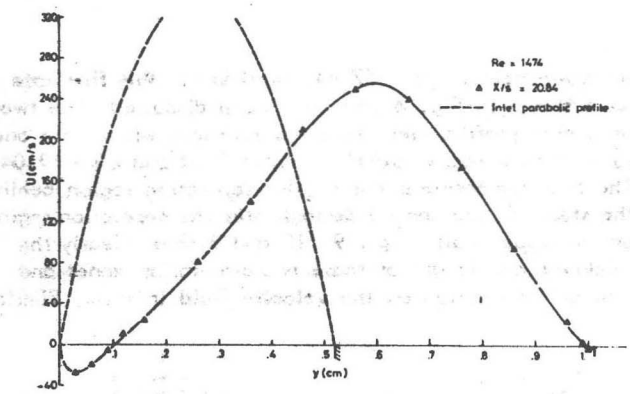


Fig. 12 Velocity profile, Re = 1474

## CONCLUSIONS

The present investigation has confirmed the strong Reynolds number dependence of the separated flow region in the immediate vicinity of a backward facing step. Separation length was measured by means of a laser-Doppler anemometer showing the strong increase with Reynolds number in the laminar flow regime and the nearly constant value in the turbulent region. Transition from laminar to turbulent flow is characterized by initially strong decrease in the main separation region which is attached to the step and also a decrease in the size of the secondary recirculating flow region which developed on the same test section wall. A recirculating flow region was also observed on the test section wall opposite to the step which decreased in size with increasing Reynolds number and decayed when the flow became fully turbulent. The axial dimensions of these flow regions are quantitatively given in the paper together with cross sectional velocity profiles to provide a picture of the flow structure downstream of the two-dimensional step.

The paper also presents preliminary prediction of the reattachment length in the laminar region and the comparison between experimental and numerical results is good. The predictions also show secondary recirculating flow region at the upper wall as observed experimentally. Refined computations are necessary, however, in order to draw any final conclusions as to agreement between measurements and predictions. The work is continued at the University of Karlsruhe.

## REFERENCES

1 Abbott, D.E. and Kline, S.J., "Experimental Investigation of Subsonic Turbulent Flow Over Single and Double Backward Facing Steps", Journal of Basic Engineering, 1962, p. 317.

2 Seban, R.A., "Heat Transfer to the Turbulent Separated Flow of Air Downstream of a Step in the Surface of a Plate", Journal of Heat Transfer, Vol. 86, No. 2, 1964, p. 259.

3 Goldstein, R.J., Eriksen, V.L., Olson, R.M. and Eckert, E.R.G., "Laminar Separation, Reattachment, and Transition of Flow over a Downstream Facing Step", Journal of Basic Engineering, 1970, p. 732.

4 Durst, F. and Whitelaw, J.H., "Aerodynamic Properties of Separated Gas Flows: Existing Measurement Techniques and New Optical Geometry for the Laser-Doppler Anemometer", Progress in Heat and Mass Transfer, Vol. 4, Pergamon Press, 1971, p. 311.

5 Gosman, A.D. and Pun, W.M., "Lecture Notes for Course Entitled : Calculation of Recirculating Flow", Heat Transfer Report HTS/74/2, 1973, Imperial College, London.

6 Denham, M.K. and Patrick, M.A., "Laminar Flow Over a Downstream-Facing Step in a Two-Dimensional Flow Channel", Trans. Instr. Chem. Engrs., Vol. 52, 1974, p. 361.

7 Etheridge, D.W. and Kemp, P.H., "Measurements of Turbulent Flow Downstream of a Rearward-Facing Step", Journal of Fluid Mechanics, Vol. 86, 1978, p. 545.

8 Wauschkuhn, P. and Ram, V.V., "Die turbulente Grenzschicht hinter einem Ablösegebiet", Zeitschrift für Flugwissenschaften, Heft 1, 23, 1975.

9 Wauschkuhn, P. and Ram, V.V., "Die turbulente Grenzschicht unmittelbar hinter dem Wiederanlegen eines Ablösegebietes", Zeitschrift für Angewandte Mathematik und Mechanik, 55, 1975.

10 Cherdron, W., Durst, F. and Whitelaw, J.H., "Asymmetric Flows and Instabilities in Symmetric Ducts with Sudden Expansions", Journal of Fluid Mechanics, Vol. 84, 1978, p. 13.

11 Durst, F. and Tropea, C., "Processing of Laser-Doppler Signals by Means of a Transient Recorder and Digital Computer, SFB 80/E/118, 1977, Sonderforschungsbereich 80, University of Karlsruhe.

12 Back, L.H. and Roschke, E.J., "Shear Layer Flow Regimes and Wave Instabilities and Reattachment Length Downstream of an Abrupt Circular Channel Expansion", Journal of Applied Mechanics, 1972, pp. 677.

13 Filetti, W.G. and Kays, W.M., "Heat Transfer in Separated Reattachment, and Redevelopment Regions Behind a Double Step at Entrance to a Flat Duct", Journal of Heat Transfer, Vol. 89, No. 2, 1967, p. 163.

14 Sparrow, E.M. and Kalejs, J.P., "Local Convective Transfer Coefficients in a Channel Downstream of a Partially Constructed Inlet", International Journal of Heat and Mass Transfer, Vol.20, No. 11, 1977, p. 1241.

# ON THE CALCULATION OF TURBULENT HEAT TRANSPORT DOWNSTREAM FROM AN ABRUPT PIPE EXPANSION

**C. C. Chieng and B. E. Launder**
Department of Mechanical Engineering
University of California,
Davis, California

## ABSTRACT

A numerical study is reported of flow and heat transfer in the separated flow region created by an abrupt pipe expansion with the standard $k-\varepsilon$ model of turbulence [1] . The study has given its main attention to the simulation of the region in the immediate vicinity of the wall where turbulent transport gives way to molecular conduction and diffusion. As in other separated flow studies, wall resistance laws or "wall functions" used to bridge this near-wall region are based on the idea that, beyond the viscous sub-layer, the turbulent length scale is universal, increasing linearly with distance from the wall. Attention to detailed modelling, however, has, it appears, produced a more satisfactory set of relations than has formerly been used. Predictions of the experimental data of Zemanick & Dougall [2] for a diameter ratio of 0.54 show generally encouraging agreement with experiment.

Nomenclature

| | |
|---|---|
| $C_{\mu\infty}, C_1, C_2$ | coefficients in turbulence model |
| $c_\ell$ | constant of proportionality between length scale $\ell$ and distance from wall (applied over near-wall cell) |
| d | diameter of pipe upstream of expansion |
| D | diameter of pipe downstream of expansion |
| $E^*$ | constant in logarithmic velocity profile (5.0) |
| $f_2, f_\mu$ | empirical functions of Reynolds number appearing in turbulence model |
| k | turbulence kinetic energy |
| $k_v$ | kinetic energy at edge of viscous sublayer |
| Nu | Nusselt number based on downstream pipe diameter |
| p | static pressure |
| r | radial coordinate |
| $Re_D$ | Reynolds number based on bulk mean velocity and diameter downstream of expansion |
| $R_t$ | turbulent Reynolds number $\rho k^2/\mu\varepsilon$ |
| $R_v$ | viscous sublayer Reynolds number (taken as a constant, 20.0) |
| T | temperature |
| U | mean velocity in x-direction |
| V | mean velocity in r-direction |
| x | coordinate parallel to pipe axis |
| y | coordinate directed radially inward with origin at pipe wall |
| $y_e$ | distance from tube wall of edge of wall adjacent cell |
| $y_v$ | viscous sublayer thickness |
| $\Gamma$ | dynamic diffusivity (thermal conductivity divided by specific heat at constant pressure) |
| $\Gamma_T$ | turbulent dynamic thermal diffusivity |
| $\varepsilon$ | dissipation rate of turbulence energy |
| $\kappa^*$ | constant in logarithmic velocity profile (0.23) |
| $\mu$ | dynamic viscosity of fluid |
| $\mu_{eff}$ | effective (i.e., turbulent + molecular) viscosity |

| | |
|---|---|
| $\mu_T$ | turbulent viscosity $C_\mu \rho k^2/\varepsilon$ |
| $\nu$ | kinematic viscosity |
| $\rho$ | density |
| $\sigma_k, \sigma_\varepsilon$ | turbulent "Prandtl numbers" for diffusion of k and ε (1.0 and 1.3) |
| $\sigma_T$ | turbulent Prandtl number (for heat transfer) (0.9) |
| $\tau$ | shear stress |
| $\tau_w$ | wall shear stress |

Subscripts

| | |
|---|---|
| e | levels prevailing at outer edge of near-wall cell |
| k,ε | values pertaining to kinetic energy and dissipation rate respectively |
| max | maximum value |
| T | denotes turbulent value of quantity |
| v | values at outer edge of viscous sublayer |
| w | wall values |

## INTRODUCTION

Several experimental studies over the past 25 years have shown that an abrupt expansion in pipe diameter or the insertion of a constriction (such as an orifice plate) in a pipe produces, on the downstream side, levels of heat transfer coefficient several times greater than that for fully developed turbulent flow at the same Reynolds number, ref. [2-6]. The reason for this heat-transfer argumentation may, in simple terms, be attributed to increases in the levels of the stream's turbulence energy, k. The crucial feature is that the blockage or expansion generates high shearing rates in *regions removed from the immediate vicinity of the pipe wall.* In such regions turbulence energy generation rates will be large (due to the high shearing) while dissipation rates will be low because, away from the wall, large scale motions predominate*. The turbulence energy level thus increases rapidly to magnitudes many times greater than commonly found in pipe flow. These elevated energies in turn lead to higher turbulent diffusion coefficients in the main (i.e., the turbulent) region of the flow and to a diminution in the thickness of the near-wall "skin" through which heat must pass largely by molecular diffusion.

An early paper by Spalding [7] recognized the main physical elements of heat transport mechanisms in separated turbulent flow; though the development path differs, two of the basic ideas from that paper are adopted in the present work. The first of these is that the wall's dominance on the length scale near the wall is complete: outside of the viscous sublayer the length scale is held to depend, for a limited region near the wall, only on the normal distance to the surface. The second is that the viscous sublayer thickness, $y_v$, adjusts itself according to the external turbulence energy such that the sublayer Reynolds number $y_v k^{\frac{1}{2}}/\nu$ is a universal constant. While these assumptions are not adequate for all types of wall flows+, they do seem to provide a good basis for analysing situations where the principal source of energy generation lies remote from the wall and thus where diffusion of energy is *towards* the surface.

A universal-length-scale treatment is of itself not adequate to model turbulent transport over the whole of a separated flow. Runchal's [8] computational studies with a fixed-length-scale model showed that, though the general dependence of heat- or mass-transfer coefficients on Reynolds number and Prandtl/Schmidt number was well predicted, the absolute level was strongly dependent on the suppositions made about the largely unguessable length scale distribution over the 90% of the flow cross-section away from the pipe wall.

The introduction, over the past decade, of two-equation models of turbulence (e.g., ref. [1]) allows, in principle, the turbulent length scale variation throughout the flow to be predicted. Such models have certainly facilitated numerical studies of turbulent recirculating flows though it must be said that agreement of such predictions with experimental data has not been uniformly satisfactory.

Nearly all previous numerical studies of separated and reattaching flows have focused on the flow field pattern, i.e., on distributions of mean velocity and, in a few cases, of turbulence energy and Reynolds stresses (e.g., ref. [9] and [10]). Now, the distribution of these parameters throughout the main part of the flow is usually only weakly dependent upon the model of turbulent transport in the immediate wall vicinity. The same is emphatically not the case, however, with the local heat transfer coefficient, computed levels being especially sensitive to the near-wall model. Three interrelated inferences may be drawn from this fact:

i) A successful numerical prediction of the flow field does not necessarily mean that the same model would give satisfactory predictions of the heat transfer coefficients along the pipe wall.

ii) In the absence of turbulence data within the viscous sublayer itself, heat transfer predictions provide the best way of refining and validating the near wall turbulence model.

iii) Refinement and validation of the near-wall model can only be made by reference to separated flows wherein the outer flow field is reasonably well predicted.

---

* It is usually supposed that, for a given turbulence energy, the energy dissipation rate varies inversely with length scale.

\+ e.g., boundary layers in strong accelerations where partial "laminarization" occurs.

These inferences shaped the scope and the details of the present exploration. The pipe-enlargement or backward-facing-step configuration appeared ideally suited for an examination of heat transfer in separated flows. The flow was (as separated flows go) reasonably simple since the separation point was fixed. Moreover, if attention is confined to large changes in diameter, the strong pressure gradients downstream of the step diminish the sensitivity of the flow field to the turbulence model employed. Thus while the k~ε viscosity model [1] under-predicts the separation length by about 30% when the step height is only a small fraction of the pipe diameter, approximately the correct reattachment length and turbulence energy levels are generated when the step height is of the order of 50% of the downstream radius. The various heat transfer studies cited above (ref. [2-6]) have all considered cases with roughly a 2:1 change in diameter. Of the available sets, we have selected those of Zemanick and Dougall [2]. The entry and boundary conditions for this flow are particularly well defined (the former being those of fully-developed pipe flow since an unheated entry length of 100 diameters preceded the expansion). Moreover, unlike the experiments taken with an orifice constriction (e.g., ref [6]) the computational domain need not extend upstream of the step itself; thus, for a given total number of grid nodes a correspondingly finer mesh could be adopted. Finally the authors have reported in great detail any shortcomings they found in their experimental data.

In the following section we develop the physical and mathematical model to be employed with particular attention to the treatment of turbulence variables in the near-wall region while in Section 3 we draw comparisons between the calculated and measured behaviour.

## MATHEMATICAL AND PHYSICAL MODEL

### The Governing Differential and Auxiliary Equations

The following set of equations, incorporating the Boussinesq turbulent-viscosity concept, is held to describe the mean velocity and temperature fields in a statistically stationary, turbulent flow through a pipe expansion.

*axial momentum*

$$\rho \frac{DU}{Dt} = -\frac{\partial p}{\partial x} + \frac{1}{r}\left[\frac{\partial}{\partial x}\left(r\,\mu_{eff}\frac{\partial U}{\partial x}\right) + \frac{\partial}{\partial r}\left(r\,\mu_{eff}\frac{\partial U}{\partial r}\right)\right] + S_u$$

$$S_u \equiv \frac{\partial}{\partial x}\left(\mu_{eff}\frac{\partial U}{\partial x}\right) + \frac{1}{r}\frac{\partial}{\partial r}\left(r\,\mu_{eff}\frac{\partial V}{\partial x}\right) \qquad (1)$$

$$\rho \frac{DV}{Dt} = -\frac{\partial p}{\partial r} + \frac{1}{r}\left[\frac{\partial}{\partial x}\left(r\,\mu_{eff}\frac{\partial V}{\partial x}\right) + \frac{\partial}{\partial r}\left(r\,\mu_{eff}\frac{\partial V}{\partial r}\right)\right] - \mu_{eff}\frac{V}{r^2} + S_v$$

$$S_v \equiv \frac{\partial}{\partial x}\left(\mu_{eff}\frac{\partial U}{\partial r}\right) + \frac{1}{r}\frac{\partial}{\partial r}\left(r\,\mu_{eff}\frac{\partial V}{\partial r}\right) - \mu_{eff}\frac{V}{r^2} \qquad (2)$$

$$\frac{\partial}{\partial x}(r\,\rho\,U) + \frac{\partial}{\partial r}(r\,\rho\,V) = 0 \qquad (3)$$

$$\rho \frac{DT}{Dt} = \frac{1}{r}\left[\frac{\partial}{\partial x}\left(r\,\Gamma_{eff}\frac{\partial T}{\partial x}\right) + \frac{\partial}{\partial r}\left(r\,\Gamma_{eff}\frac{\partial T}{\partial r}\right)\right] \qquad (4)$$

The effective turbulent viscosity is obtained from the k~ε viscosity model of Jones & Launder [1]. Two forms have been employed: the "high-Reynolds-number" form has been adopted for the majority of the tests while, for one set of conditions, a solution has been obtained, using a highly compressed grid near the wall, to the complete low-Reynolds number form of the model. In the composite form given below terms appearing in boxes are omitted in the high Reynolds number version of the model:

$$\mu_{eff} = \mu + \mu_T \quad ; \quad \mu_T = C_{\mu\infty}\,\boxed{f_\mu}\,\rho k^2/\varepsilon$$

$$\Gamma_{eff} = \Gamma + \Gamma_T \quad ; \quad \Gamma_T = \mu_T/\sigma_T \quad (\sigma_T = 0.90) \qquad (5)$$

$$\rho \frac{Dk}{Dt} = \frac{1}{r}\left[\frac{\partial}{\partial x}\left(r\left(\mu + \frac{\mu_T}{\sigma_k}\right)\frac{\partial k}{\partial x}\right) + \frac{\partial}{\partial r}\left(r\left(\mu + \frac{\mu_T}{\sigma_k}\right)\frac{\partial k}{\partial r}\right)\right]$$

$$+ \mu_T\left\{\left(\frac{\partial U}{\partial r} + \frac{\partial V}{\partial x}\right)^2 + 2\left(\frac{\partial U}{\partial x}\right)^2 + 2\left(\frac{\partial V}{\partial r}\right)^2 + \left(\frac{V}{r}\right)^2\right\}$$

$$- \rho\varepsilon\,\boxed{- 2\mu\left(\frac{\partial k^{1/2}}{\partial r}\right)^2} \qquad (6)$$

$$\rho \frac{D\varepsilon}{Dt} = \frac{1}{r}\left[\frac{\partial}{\partial x}\left(r\left(\mu + \frac{\sigma_T}{\sigma_\varepsilon}\right)\frac{\partial \varepsilon}{\partial x}\right) + \frac{\partial}{\partial r}\left(r\left(\mu + \frac{\mu_T}{\sigma_\varepsilon}\right)\frac{\partial \varepsilon}{\partial r}\right)\right]$$

$$+ C_1\frac{\varepsilon}{k}\mu_T\left\{\left(\frac{\partial U}{\partial r} + \frac{\partial V}{\partial x}\right)^2 + 2\left(\frac{\partial U}{\partial x}\right)^2 + 2\left(\frac{\partial V}{\partial r}\right)^2 + \left(\frac{V}{r}\right)^2\right\}$$

$$- C_2\,\rho\frac{\varepsilon^2}{k}\,\boxed{f_2} \quad + \quad \boxed{2.0\,\frac{\mu\,\mu_T}{\rho}\left(\frac{\partial^2 U}{\partial r^2}\right)^2} \qquad (7)$$

where the asymptotic, high-Reynolds-number values of the coefficients are:

| $C_{\mu\infty}$ | $C_2$ | $C_1$ | $\sigma_k$ | $\sigma_\varepsilon$ |
|---|---|---|---|---|
| 0.09 | 1.92 | 1.44 | 1.0 | 1.3 |

and, following the reoptimization by Launder & Sharma [11], the low-Reynolds-number functions are taken as:

$$f_\mu = \exp\left(-\frac{3.4}{(1+R_t/50)^2}\right) \quad \text{where} \quad R_t = \frac{\rho k^2}{\varepsilon\mu}$$

$$f_2 = 1.0 - \frac{0.4}{1.8}\exp -(R_t/6)^2 \ .$$

When the low Reynolds number form of the model is used, the boundary conditions $k = 0$ and $\varepsilon = 0$† are applied at the wall itself. With the high Reynolds number formulation, levels of *near*-wall kinetic energies and dissipation rates are obtained as described in the following sub-section.

## Near-Wall Model for High Reynolds Numbers

The detailed handling of the near-wall region is at least partly shaped by the methodology of the finite-difference procedure. With the TEACH series of programs, the set of difference equations linking the value of a dependent variable at one node with those at its neighbors is obtained by integration of the governing equation (or, equivalently, by application of the basic physical transport law) over a control volume surrounding each node. The control volume boundaries bisect perpendicularly the lines joining adjacent nodes so that when – as here – the problem involves only rectilinear surfaces, the edges of the solution domain coincide with control volume boundaries. Figure 1a shows a scalar node P whose associated volume is bounded on the west side by a wall. The near wall-flow is treated as viscous (but not laminar) out to a distance $y_v$ from the wall and fully turbulent beyond this. The sublayer thickness $y_v$ is such that the Reynolds number $y_v k_v^{\frac{1}{2}}/\nu (\equiv R_v)$ is a constant, taken equal to 20. Note that from figure 1a the near-wall cell is large enough that the node P lies outside of the viscous sublayer. For the purpose of estimating the frictional force applied at the wall we need a connection between the velocity at node P and the wall shear stress $\tau_w$. Over the fully turbulent region the mean velocity parallel to the wall is assumed to vary with height according to

$$\frac{U k_v^{\frac{1}{2}}}{(\tau_w/\rho)} = \frac{1}{\kappa^*} \ell n\, E^* \frac{y k_v^{\frac{1}{2}}}{\nu} \qquad (8)$$

which, on inverting and evaluating the resultant expression at node P gives:

$$\tau_w = \kappa^* \rho\, U_p k_v^{\frac{1}{2}} / (\ell n\, E^* y_p k_v^{\frac{1}{2}}/\nu) \qquad (9)$$

Equations (8) and (9) are the same as proposed in Launder & Spalding [12] except that the kinetic energy term is here evaluated at the edge of the viscous sublayer rather than at node P. The quantity $\kappa^*$ in (8) is proportional to the von Karman constant, $\kappa$. In local equilibrium where $k = (\tau_w/\rho) C_{\mu\infty}^{-\frac{1}{2}}$ the velocity relation should reduce to the conventional logarithmic law:

$$\frac{U}{\sqrt{\tau_w/\rho}} = \frac{1}{\kappa} \ell n\, E\, y \sqrt{(\tau_w/\rho)}/\nu \qquad (10)$$

† For an explanation of this boundary condition see Jones & Launder [1].

This limiting form is achieved by taking $\kappa^* = \kappa C_{\mu\infty}^{\frac{1}{4}}$ (0.23) and $E = E^* C_{\mu\infty}^{-\frac{1}{4}}$. The constant $E^*$ can be evaluated in terms of $R_v$ by noting that within the viscous sublayer the velocity displays a linear variation which we may write as:

$$\frac{U k_v^{\frac{1}{2}}}{\tau_w/\rho} = \frac{y k_v^{\frac{1}{2}}}{\nu} \qquad (11)$$

On equating the velocities given by (8) and (11) at $y_v$ we find:

$$E^* = \exp(\kappa^* R_v)/R_v \ ,$$

thus, for the quoted values of $\kappa^*$ and $R_v$, $E^* = 5.0$.

Let us now consider the question of formulating the budget of the turbulence energy over a wall-adjacent cell. In physical terms equation (6) expresses a balance between convective transport, diffusion generation and destruction. The convection terms, which will generally be of minor influence near the wall, are handled in an entirely standard way, all fluid leaving the cell being supposed to have the energy at node P. The diffusion treatment becomes evident once the general variation of turbulence energy over the cell is fixed. The assumed distribution is shown in figure 1b: the linear variation between nodes P and its eastern neighbor is considered to extrapolate to the edge of the viscous sublayer (thus fixing $k_v$ in terms of $k_P$, $k_E$ and the relevant geometric dimensions). Within the viscous layer a parabolic variation of kinetic energy is assumed:

$$k = k_v (y/y_v)^2 \ , \qquad (12)$$

which corresponds to a linear increase of fluctuating velocity with distance from the wall. Note that since k has zero gradient at the wall there is no diffusional "leakage" of kinetic energy to the surface. The diffusional flux of energy out of (or, more usually, into) this cell at its east boundary is handled by the same conservative differencing scheme that is employed over the remainder of the flow; the diffusive transport through the north and south boundaries is likewise handled by the standard procedure.

The evaluation of the appropriate mean rates of generation and dissipation over the cell requires a little more care. The dominant contribution to the energy generation rate is the term $\tau_T \partial U/\partial y$, $\tau_T$ being the local turbulent shear stress. The assumed variation of this quantity is shown in figure 1c: the stress is zero within the viscous sublayer, undergoes an abrupt increase at the edge of the sublayer and varies linearly over the remainder of the cell. The precise form of this linear variation is fixed by connecting the turbulent shear stress at the outer edge of the cell $\tau_e$ with the wall stress, $\tau_w$. The mean generation rate per unit volume is thus: